Temperature-Induced Changes in Protein Structures Studied by Fourier Transform Infrared Spectroscopy and Global Analysis†

I. H. M. van Stokkum,*,‡ H. Linsdell,§ J. M. Hadden,§ P. I. Haris,§ D. Chapman,§ and M. Bloemendal*,‡,§

Faculty of Physics and Astronomy, Vrije Universiteit, Amsterdam, The Netherlands, and Department of Protein and Molecular Biology, Royal Free Hospital School of Medicine, London, U.K.

Received August 24, 1994; Revised Manuscript Received April 10, 1995⊗

ABSTRACT: Fourier transform infrared (FTIR) spectroscopy has been used to study temperature-induced structural changes which occur in albumin, immunoglobulin G, fibrinogen, lysozyme, α-lactalbumin, and ribonuclease S when dissolved in ^2H_2O. In order to analyze the data, a new method was developed in which the data were analyzed globally with the aid of a spectral model. Seven or eight bands were sufficient to fit the full data set of spectra ranging from 1420 to 1760 cm^{-1} with a root mean square error of 1−2% of the maximum. Subsequently, the estimated band amplitude curves which showed a sigmoidal progression with increasing temperature were (globally) fitted with a two-state thermodynamic model. In this way, information on structural changes as well as on the thermal stability of the proteins was obtained. In all proteins investigated, enhanced $^1H-^2H$ exchange occurred at temperatures well below the unfolding of the secondary structure. This was interpreted as a change in tertiary structure leading to enhanced solvent accessibility. In all the proteins investigated, except for ribonuclease S, an intermolecular β-sheet band indicative of aggregation appeared concomitant with the denaturation of the secondary structure. The results are compared with data from other techniques and discussed in terms of local unfolding and folding intermediates.

It is generally accepted that transient partly folded states are responsible for the rapidity of folding of proteins (Creighton, 1994). Nevertheless, the precise mechanism of protein folding and unfolding is still a matter of great debate (Baldwin, 1990; Ptitsyn et al., 1990; Buchner et al., 1991; Pain, 1992; Creighton, 1994; Sosnick et al., 1994). It has been suggested that as many different techniques as possible should be applied to a given protein to reach unambiguous conclusions on the conformational changes during protein folding (Pain, 1992). Folding intermediates have now been studied by circular dichroism, fluorescence, differential scanning calorimetry, two-dimensional nuclear magnetic resonance, X-ray scattering, Raman spectroscopy and molecular dynamics [see, e.g., Lin and Koenig (1976), Dolgikh et al. (1981), Kuwajima et al. (1985), Miranker et al. (1991), Xie et al. (1991), Lala and Kaul (1992), and Mark and van Gunsteren (1992)].

A technique widely used nowadays to study protein structure is Fourier transform infrared (FTIR)[1] spectroscopy. For reviews see Susi and Byler (1986), Haris and Chapman (1992), Surewicz et al. (1993), and Arrondo et al. (1993). Protein conformational stability can be studied spectroscopically by monitoring the spectra as a function of temperature (or of another denaturation parameter) (Pace et al., 1989). Examples using FTIR spectroscopy are Clark et al. (1981), Yang et al. (1987), Casal et al. (1988), Kirsch and Koenig (1989), Muga et al. (1991), and Hadden et al. (1994a,b). In these cases transitions in the amide I/I′ region are observed which are discussed mainly qualitatively by monitoring the value at one or more representative wavenumbers. Several techniques are used to resolve the heavily overlapping FTIR absorption bands: differentiation, Fourier self-deconvolution, and curve fitting [for reviews see Susi and Byler (1986) and Arrondo et al. (1993)]. As yet these techniques are less suitable to analyze spectra as a function of a variable. Therefore we introduce here a new global analysis method, which combines curve fitting with linking of the spectral shape parameters across the variable parameter, in this case temperature (Van Stokkum et al., 1994). It is implicitly assumed that the spectral shape is independent of temperature. In contrast to differentiation and Fourier self-deconvolution, direct least-squares fitting of the spectra is less sensitive to additive random noise and no information is lost (Arrondo et al., 1993). However, the limitation of curve fitting lies in the need to assume a specific band shape. The model-based parameter estimation presented here allows evaluation of the fit quality according to statistical criteria, e.g., residuals and standard errors of the parameters.

Thus we studied temperature-induced structural changes of albumin (ALB), immunoglobulin G (IgG), fibrinogen (FIB), lysozyme (LYS), α-lactalbumin (LAC), and ribonuclease S (RIB) in ^2H_2O buffer by means of FTIR spectroscopy. ^2H_2O was used instead of H_2O, as this allowed us to use longer path lengths, which helps to reduce any possible effects of solvent evaporation and also results in a higher signal-to-noise ratio. In addition, hydrogen−deuterium exchange of undeuterated protein in ^2H_2O can provide information on enhanced solvent accessibility and/or local unfolding and hence on conformational changes which occur

† Financially supported by the Interdisciplinary Research Centre for Biomedical Materials [H.L., P.I.H., D.C., and M.B.].

* Address correspondence to either of these authors at the Faculty of Physics and Astronomy, Vrije Universiteit, De Boelelaan 1081, 1081 HV Amsterdam, The Netherlands.

‡ Vrije Universiteit.

§ Royal Free Hospital School of Medicine.

⊗ Abstract published in *Advance ACS Abstracts,* August 1, 1995.

[1] Abbreviations: ALB, albumin; IgG, immunoglobulin G; FIB, fibrinogen; FTIR, Fourier transform infrared; LYS, lysozyme; LAC, α-lactalbumin; RIB, ribonuclease S.

0006-2960/95/0434-10508$09.00/0

(Wedin et al., 1982; Englander & Kallenbach, 1984; Rashin, 1987; Miranker et al., 1991; Haris & Chapman, 1992). The amide II/II′ band is a particularly good probe of this exchange process as it shifts from about 1550 (amide II) to 1450 cm^{-1} (amide II′). The major plasma proteins ALB, IgG, and FIB were selected for this study because the first two are single-chain, essentially α-helical and β-sheet proteins, respectively, while fibrinogen is an example of a multisubunit protein with a complicated tertiary and quaternary structure (Procyk et al., 1992). Moreover, the conformation and conformational changes in IgG and FIB are of interest for research on biomedical materials due to their role in immunoresponse and blood clotting, respectively (Igarashi et al., 1990; Azpiazu & Chapman, 1992). LAC and LYS are closely related proteins that have been extensively studied for folding intermediates but appear to have rather different folding behavior notwithstanding their close homology (Kuwajima et al., 1985; McKenzie & White, 1991). The set was completed with RIB, as this is a protein that is generally fully reversible after thermal denaturation (Haris et al., 1986).

Two types of model were used to analyze the data. First the data were analyzed globally with the help of a spectral model in which the spectra are described as a sum of skewed Gaussian bands, whose amplitudes as a function of temperature are called band-amplitude curves. Second the estimated band-amplitude curves which showed a sigmoidal progression with increasing temperature were fitted with a two-state thermodynamic model. Thus we extracted information on structural changes and on the thermal stability of the proteins. The structure of the rest of this paper is as follows. After a description of the experimental procedures, the global analysis method will be explained. Then follows a phenomenological description of the spectra and band assignment. The results from the global analysis are presented in two wavenumber ranges, ending with the thermodynamic fit of the band-amplitude curves. In the Discussion we compare the outcome of the global analysis method with existing methods and interpret our results with respect to protein structural changes.

MATERIALS AND METHODS

Proteins. Bovine pancreas ribonuclease S (R6000), human α-lactalbumin (L7269), human serum albumin (A3782), hen egg white lysozyme (L6876), human immunoglobulin G (I4506), and human fibrinogen (F4129) were obtained from Sigma (Poole, U.K.) and used without further purification. Deuterium oxide (99.8% ^2H) was also obtained from Sigma.

Experimental Procedures. Proteins were dissolved at a concentration of about 20 mg/mL in ^2H_2O buffer containing phosphate-buffered saline prepared from tablets (Sigma P-4417). FTIR spectra were recorded using a Nicolet 740 spectrometer. Samples were placed in a microcell consisting of two CaF_2 windows and a 50-μm Teflon spacer. A sample shuttle (shuttling every 5 scans) was employed for signal averaging of the sample with the background. Double-sided interferograms were apodized with a Happ−Genzel function (Griffiths & Haseth, 1986) prior to further transformation of the data. All spectra were recorded at a resolution of 2 cm^{-1}. Forty scans were signal-averaged per measurement. Temperature, monitored by means of a thermocouple attached to the cell, was varied from 14 to 82 °C and then back to 15 °C. Below 50 °C, spectra were recorded at intervals of 2−5 °C, whereas above this temperature the intervals were 1−2 °C. In this a total of 74 spectra were recorded in an experiment of approximately 8 h. Buffer spectra were recorded under identical conditions as the sample spectra. The spectrometer was continuously purged with dry air to eliminate contributions from water-vapor absorption. For subtraction, a buffer containing 1% ^1H_2O was used. Buffer subtraction was carried out automatically using two criteria. First, the spectrum in the 1900−1740-cm^{-1} region was fitted with a baseline plus a constant times the buffer spectrum. Since this procedure resulted in fluctuations, particularly below 1600 cm^{-1}, an extra point at 1517 cm^{-1} (the maximum of the tyrosine band) with a relative weight of 50 was added to the above-mentioned linear regression fit in order to keep this band's amplitude approximately constant.

For assignment of bands, the spectra were analyzed using second derivatives and Fourier self-deconvolution. Second-derivative spectra were calculated over a 13-cm^{-1} range using a 13-data-point Savitzky−Golay smoothing window. Deconvolution was performed with band widths between 12 and 16 cm^{-1} and resolution enhancement factors between 1.7 and 2.2. Further details can be found in Hadden et al. (1994a).

Global Analysis. The FTIR spectra (74 in total) measured at different temperatures were analyzed globally using a single model function to describe all data. Thus the information contained in the noisy data is condensed into a small number of parameters which are estimated more precisely. The adequacy of the model is judged from the size and structure of the residuals. According to the superposition principle the (noise-free) model function of the protein FTIR spectrum $\gamma(\bar{\nu}, T)$ measured at wavenumber $\bar{\nu}$ and temperature T is given by

$$\gamma(\bar{\nu}, T) = \sum_{k=1}^{N} c_k(T)\, \epsilon_k(\bar{\nu}) \qquad (1)$$

where the sum extends over N absorption bands, with index k, which we assume to be independent of temperature. $\epsilon_k(\bar{\nu})$ is the shape of absorption band k, which may be characteristic for a particular secondary-structure class or a particular amino-acid side chain. $c_k(T)$ is the amplitude of this band k, possibly dependent upon temperature.

Decomposition of $\gamma(\bar{\nu}, T)$ into N (linearly independent) pairs $c_k(T)$, $\epsilon_k(\bar{\nu})$ requires a model for either c or ϵ. Here we use a spectral model (Van Stokkum et al., 1994) assuming a skewed Gaussian shape (Fraser & Suzuki, 1969; Sevilla et al., 1989) which depends upon three parameters: location $\bar{\nu}_{max}$, width $\Delta\bar{\nu}$, and skewness b:

$$\frac{\epsilon(\bar{\nu})}{\bar{\nu}} = \exp\left(-\ln 2 \left[\frac{\ln(1 + 2b(\bar{\nu} - \bar{\nu}_{max})/\Delta\bar{\nu})}{b}\right]^2\right) \qquad (2)$$

Note that, with skewness parameter $b = 0$, eq 2 reduces to a normal Gaussian (since $\lim_{b\to 0} [\ln(1 + bx)]/b = x$). The full width at half-maximum (fwhm) is given by $\Delta\bar{\nu}_{1/2} = \Delta\bar{\nu}\ \sinh(b)/b$. The estimated band amplitudes $\hat{c}_k(T)$ should be nonnegative; otherwise the fit is unsatisfactory.

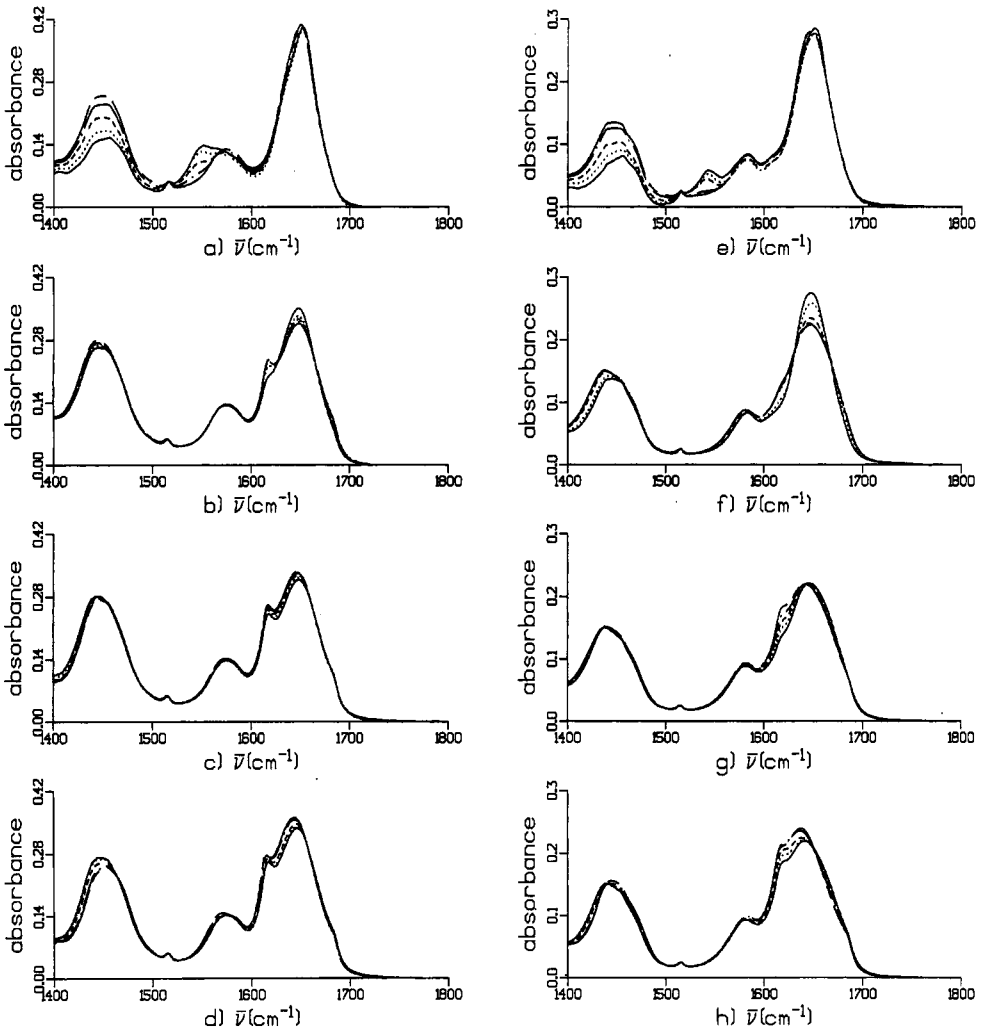

FIGURE 1: FTIR spectra of ALB (a−d) and LYS (e−h) as a function of temperature. Parts (a,b) and (e,f) represent the heating phase, whereas parts (c,d) and (g,h) represent the cooling phase. Temperatures (°C) and line types: (a, e) 14 (solid), 27 (dotted), 43 (dashed), 52 (dot dashed), 57 (chain dashed): (b, f) 64, 68, 72, 76, 79; (c, g) 82, 78, 72, 67, 62; (d, h) 60, 54, 43, 25, 15.

After a satisfactory fit with this global analysis using a spectral model, the next step is to extract the thermodynamic information. The estimated $\hat{c}_k$ (T) curves, which show a sigmoidal progression, are fitted with a thermodynamic model which we adopted from Elwell and Schellman (1977) and Pace et al. (1989). Assuming a two-state mechanism for a certain band, the sigmoidal curve is parameterized by

$$c\,(T) = c_U + \frac{c_F - c_U}{1 + \exp\left(-\frac{\Delta H_m}{R}\left(\frac{1}{T} - \frac{1}{T_m}\right)\right)} \qquad (3)$$

where c_F and c_U are the band amplitudes before and after the transition. T_m is the midpoint of the sigmoidal curve, ΔH_m is the apparent enthalpy change at T_m, and R is the gas constant. We assume a temperature-independent (van't Hoff) enthalpy ΔH and neglect here heat-capacity changes. Thus the sigmoidal curve depends upon only four parameters: c_F, c_U, T_m, and ΔH_m. When multiple c (T) curves are globally analyzed, the parameters T_m and ΔH_m are linked, whereas the parameters c_F and c_U vary. All parameters were estimated by means of a nonlinear least-squares fit, details of which are described in Van Stokkum et al. (1994).

RESULTS

Spectra and Band Assignment. In Figure 1 the FTIR spectra of ALB (a−d) and LYS (e−h) are shown as a function of temperature. In the first part of the heating phase (Figure 1a,e) there are clear indications for hydrogen−deuterium exchange. The amide II band around 1545 cm^{-1} collapses, whereas the amide II′ band around 1445 cm^{-1} [which overlaps with the HO^{2}H bending mode (Zuber et al., 1992)] increases in intensity. Only minor changes in the amide I/I′ region (1600−1720 cm^{-1}) are visible. In the second part of the heating phase (Figure 1b,f) this amide I/I′ region shows pronounced changes: the peak around 1650 cm^{-1} decreases, whereas a peak around 1620 cm^{-1} increases. The decrease around 1650 cm^{-1} is attributed to a change in the secondary structure. The rise of the peak around 1620 cm^{-1} is most likely due to intermolecular β-sheet formation (Clark et al., 1981; Yang et al., 1987; Arrondo et al., 1993). During the cooling phase, small changes are present for ALB (c,d), whereas in the case of LYS (g,h), the band around 1620 cm^{-1} continues to rise, indicative of further aggregation.

Table 1 summarizes the band maxima as obtained from second derivative and deconvoluted spectra, with column headings 14 and 82 indicating the temperatures during heating. From 1600 to 1700 cm^{-1} a total of eight band positions can be discriminated. Between 1600 and 1614 cm^{-1} a minor band is observed due to side-chain vibrations; between 1616 and 1620 cm^{-1} a band is found at high temperature that is caused by intermolecular β-sheet forma-

Table 1: Band Maxima Found from Second Derivative/Deconvolution and Global Analysis[a]

ALB			FIB			IgG			LAC			LYS			RIB		
14	82	glob	14	82	glob	14	82	glob	14	82	glob	14	82	glob	14	82	glob
1516	1516	1516	1515	1515	1516	1515	1515	1516	1516	1516	1516	1515	1515	1516	1516	1515	1516
1531	1531		1530	1530					*1530*	*1530*		1530	1530		1530		
1550		1545			1545			1545	1548		1545	1550		1545	1547		1545
1568	1572		1566	1572		1563	1568								1563	*1566*	
1584	*1584*	1577	1586		1578	1584	*1573*	1580	1585	1585	1580	1585	1578	1586	1584	1583	1584
1612	*1606*		1608	*1606*		1612	*1600*		1614			1609	1602		1608	1612	
	1616	1617		1616	1617		1620	1620		1616	1619		1618	1619			1625
1632			1639			1637		1638	1633		1639	1638		1639	1636		1635
	1650	1649		1648	1642		1646			1650	1651		1640			1647	
1654			1653					1659	1651			1655		1656	*1655*		1654
					1665	*1662*			1662						1664		
			1672			1671					1677	1673		1669		*1673*	1674
1680	1684	1678	1687	1683		1688			*1680*	*1682*		1688	1685		1687		

[a] 14 and 82 mean combination of second derivative and deconvolution at 14 and 82 °C (during heating), respectively; glob is from global analysis of the total temperature range. Italic type means not obvious from both second derivative and deconvolution. Band maxima are given in reciprocal centimeters.

tion upon aggregation; the intramolecular β-sheet band is positioned between 1632 and 1639 cm^{-1}; at higher temperatures the random coil band is located between 1640 and 1650 cm^{-1}; between 1651 and 1655 cm^{-1} α-helix absorbs; in some cases a band is found at 1662 cm^{-1} that might be due to turns or 3_{10}-helix; between 1671 and 1673 cm^{-1} another turn absorption is observed; and between 1680 and 1688 cm^{-1} the high-energy band of β-sheet structures is found [assignments based on Clark et al. (1981), Haris et al. (1986), Yang et al. (1987), Casal et al. (1988), Prestrelski et al. (1991a,b), and Arrondo et al. (1993)].

Global Analysis. In order to quantify the qualitative observations, the data were analyzed globally using the minimum number of bands necessary for a reasonable fit with nonnegative band amplitudes. As a consequence, strongly overlapping bands with the same amplitude variation as a function of temperature were fitted with a single (skewed) band. Although this has the disadvantages that (a) in some cases the change in different secondary-structure elements is not separately monitored and (b) minor bands may be neglected altogether, it prevents the introduction of artifacts due to overfitting of the data. Seven or eight bands were sufficient to achieve a fit with a root mean square error of 1−2% of the peak and largest deviations less than 8%. Examples of the residuals, which still show some structure, are given in Figure 2. These residuals will be discussed in subsequent sections. Taking into account the uncertainty caused by the buffer subtraction procedure, the fit was considered satisfactory.

Two symmetric band shapes (Gaussian and Lorentzian) were also tested in the spectral model. In general the results were comparable; however, the residuals were somewhat larger when a skewness parameter is lacking. The heavy tails of the Lorentzian resulted in larger overlap, thereby causing more negative amplitudes. Thus the skewed Gaussian band shape was used for this study.

In Figure 3 the decompositions of the temperature-resolved FTIR spectra resulting from a global analysis with the help of the spectral model (eqs 1 and 2) are depicted. Each row represents a different protein. In the last column the fitted bands are shown, which are distinguished by different symbols. The accompanying band amplitudes are shown in the left (1420−1600 cm^{-1}) and middle (1600−1720 cm^{-1}) columns. The errors in these amplitudes (indicated by vertical bars) are in general small. All spectral parameters are compiled in Table 1S of the supporting information; the peak maxima are also given in Table 1 (columns headed glob).

1420−1600-cm^{-1} Range. We will first discuss the bands below 1600 cm^{-1} (whose amplitudes are depicted in the left column of Figure 3). We chose to fit the 1420−1515-cm^{-1} region with a single (skewed) band (△) containing the amide II′ band, the HO^2H bending mode, and side-chain contributions, as a satisfactory decomposition was not always possible. It can be seen from Figures 1 and 2 that some changes in this region cannot be captured with this single temperature-independent band shape, in particular a shift to higher wavenumbers upon cooling. The band around 1516 cm^{-1} (□) is pronouncedly present in all spectra and is assigned to tyrosine side chain. The parameters of this band and of the amide II band around 1545 cm^{-1} (○) were estimated from a restricted wavenumber-region fit and kept fixed during the full analysis. Although the second-derivative and deconvoluted spectra in some cases showed multiple amide II bands (Table 1), we did not attempt to decompose the spectrum in the amide II region into smaller bands, for the reasons outlined above. A band near 1580 cm^{-1} arises from the carboxylate group (+) [e.g., Chirgadze et al. (1975) and Venyaminov and Kalnin (1990)]. This band is skewed toward higher energies. This might be explained by the contributions from two amino acids, glutamic acid and aspartic acid, as well as by minor absorption bands of side chains around 1600 cm^{-1}. Indeed, second derivative and deconvoluted spectra contain two or three strongly overlapping bands in this region (Table 1). In some cases (FIB, IgG) the band has some structure around and above 1700 cm^{-1}. This may be due to COO^2H groups (Chirgadze et al., 1975; Casal et al., 1988). The tyrosine (□) and carboxylate (+) band amplitudes remain more or less constant during heating and cooling. Slight changes are attributed to inaccuracies in the measurements or in the buffer subtraction. The amplitudes of the amide II (○) and amide II′ (△) bands behave complementarily. This confirms the above-described interpretation in terms of $^1H-^2H$ exchange.

1600−1720-cm^{-1} Range. In the region from 1600 to 1720 cm^{-1}, at least three bands were identified for each protein by the global analysis (amplitudes of which are depicted in the middle column of Figure 3). The main contribution to

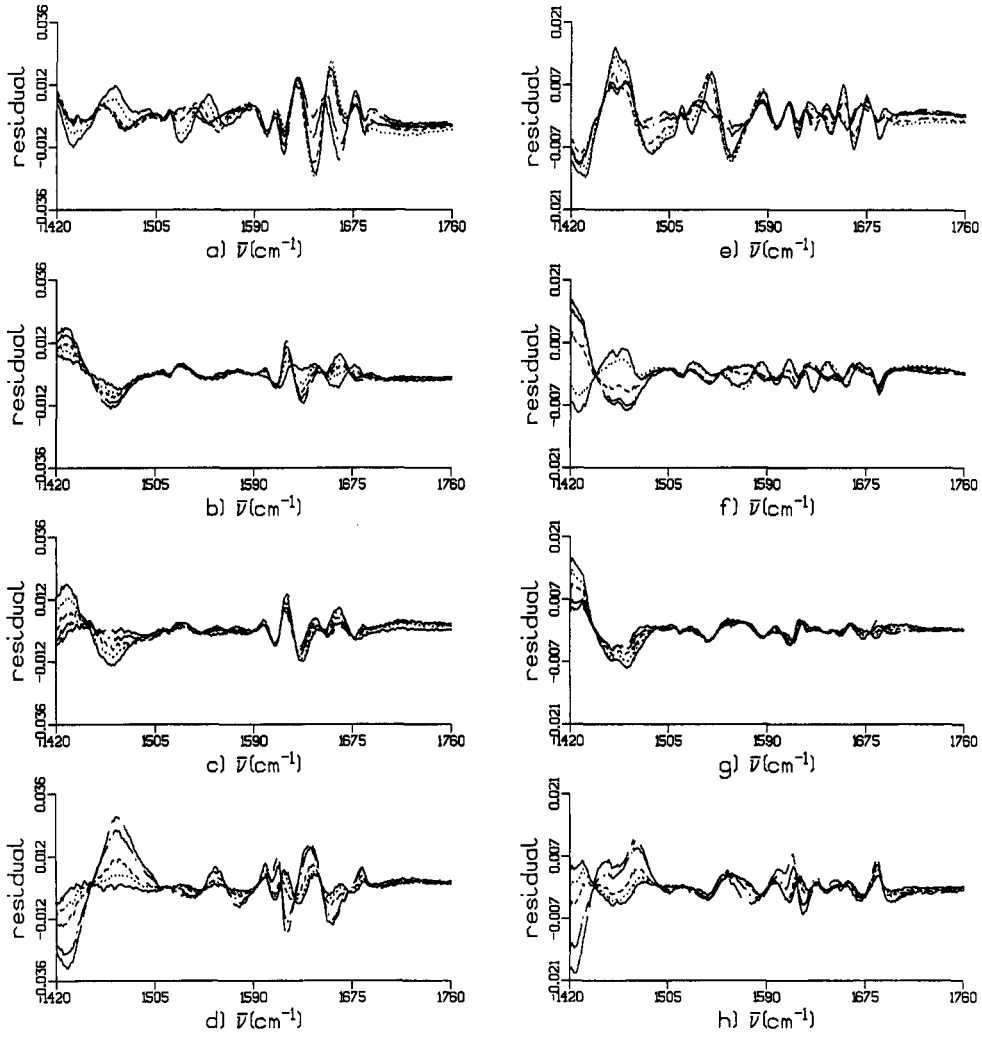

FIGURE 2: Residuals of global analysis of FTIR spectra of ALB (a–d) and LYS (e–h). Format is the same as in Figure 1.

the FTIR spectra in this range is the amide I/I′ band which is strongly dominated by the C=O stretch vibration that is highly sensitive to the secondary structure. Interpretation of results related to conformational changes in ^2H_2O may be obscured by enhanced $^1H-^2H$ exchange upon unfolding of the protein leading to band shifts. However, except for the weak high-frequency band of the antiparallel β-sheet and the band due to unordered structure, these shifts are generally relatively small (2–5 cm^{-1}; Arrondo et al., 1993). Nevertheless, exchange-induced band shift should always be considered and may affect results, as will be discussed below for LAC and LYS. The residuals in this region (Figure 2) may also be due to the effect of $^1H-^2H$ exchange.

As Figure 3 shows, some general features can be observed. All proteins except RIB have a low-frequency band (indicated by ×) between 1617 and 1620 cm^{-1} that shows an upward transition upon heating, most likely due to intermolecular β-sheet formation and molecular aggregation. In ALB, IgG, LAC, and LYS (Figure 3b,h,k,n) the amplitude is constant during the heating after the transition. Upon cooling there is a further increase in this band's amplitude, which is also the case for FIB (Figure 3e). Cooling apparently enhances the intermolecular β-sheet formation. One would expect that at low temperature (before heating) no intermolecular β-sheet would be observed. Nevertheless it can be seen from Figure 3h,n that for IgG and LYS the amplitude of the 1620-cm^{-1} band deviates considerably from zero before the heating started. The presence of a β-sheet-like structure with hydrogen bonding to another type of structure (Arrondo et al., 1993) or nonbonded β-sheet (Casal et al., 1988) may be responsible for this. Also, side-chain absorptions may contribute. Alternatively, some of the protein may be aggregated in advance.

The next three bands in the deconvoluted and second-derivative spectra (β-sheet 1632–1639 cm^{-1}, random coil 1646–1650 cm^{-1}, and α-helix 1651–1655 cm^{-1}; see Table 1) are combined into a single band (indicated by ◇) for ALB, FIB, and IgG (Figure 3b,e,g). The amplitude of this band decreases upon heating. The frequency of its maximum is 1649 and 1638 cm^{-1} for the predominantly α-helical and β-sheet proteins ALB and IgG, respectively. For FIB, whose secondary structure is still a matter of debate (Pandya et al., 1985; Azpiazu & Chapman, 1992), an intermediate value of 1642 cm^{-1} is found. We consider this band as representative for the native secondary structure. The absence of an increasing random-coil band upon denaturation can be explained by the coincidence of secondary-structure unfolding and aggregation (middle column of Figure 3). For LAC and LYS, two proteins with mixed secondary structure (Levitt & Greer, 1977; Ewbank & Creighton, 1993a), global analysis resolves two bands between 1639 and 1656 cm^{-1} (Figure 3l,o). The band at 1639/1640 cm^{-1} (◇) is presumably due to intramolecular β-sheet, and the band at 1651/1656 cm^{-1} (▽), to α-helix. A consequence of the extra band is increased

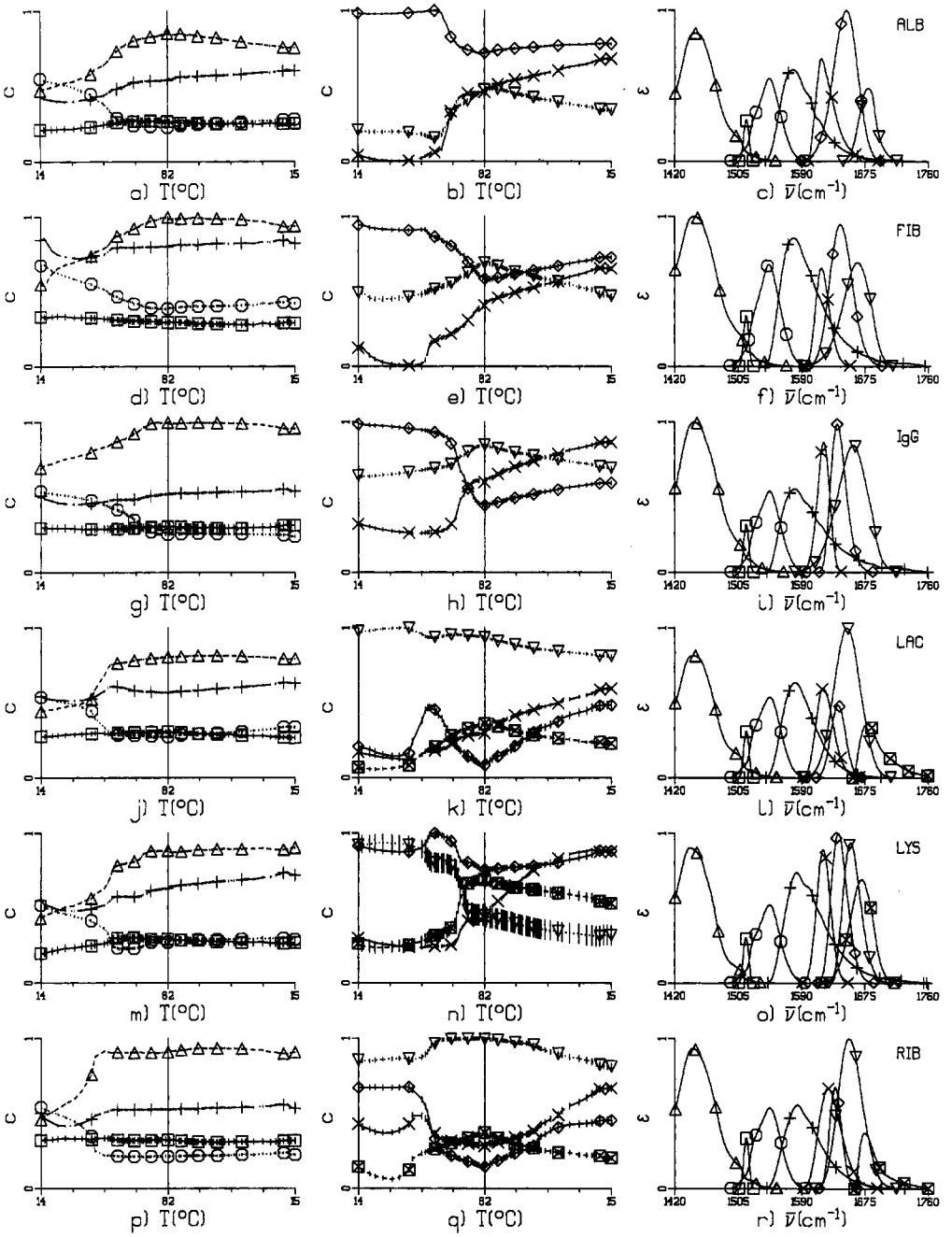

FIGURE 3: Decompositions of the temperature-resolved FTIR spectra resulting from global analysis with the help of a spectral model. Different rows represent proteins, from top to bottom: ALB, FIB, IgG, LAC, LYS, and RIB. Right column depicts fitted bands distinguished by different symbols. The spectral parameters of the bands are compiled in Table 1S in the supporting information. The accompanying band amplitudes are drawn in the left and middle column, distinguished by line types and symbols referring to the bands in the right column (vertical bars indicate ± standard error). Regarding the scaling in a row: since the product $c_k(T)\,\epsilon_k(\bar{\nu})$ is estimated, we calculate the maximum of this product per band and determine the band with the largest maximum. The c_k and ϵ_k maxima of this band are arbitrarily set at unity. The other bands are scaled relative to this band, e.g., a maximum of 0.8 in c and ϵ corresponds to a relative $c_k\epsilon_k$ maximum of 0.64. The curves are thus scaled according to their contribution to $\gamma(\bar{\nu}, T)$. For further explanation see text.

band overlap, which in the case of LYS results in quite large standard errors of some of the band amplitudes (▽ in Figure 3n,o). The β-sheet band (◇) shows an initial sigmoidal increase followed by an also sigmoidal decrease. As the temperatures of the upward transition coincide with those of the decrease in amide II and increase in amide II′ band described in the previous section, we assign this to $^1H-^2H$ exchange leading to band shift. The decreasing transition is concomitant with aggregation and the formation of intermolecular β-sheet. The α-helix (▽) band shows a slight decrease at the exchange temperature, followed in the case of LYS by a pronounced transition at the temperature where the β-sheet denatures and the protein aggregates. The interpretation of the lower temperature change in terms of $^1H-^2H$ exchange is supported by measurements in ^1H_2O (unpublished results), where only the high-temperature transitions are found.

The high-frequency part of the amide I/I′ region is described in the global analysis by a single band with a frequency between 1659 and 1678 cm^{-1} (▽ for ALB, IgG, and FIB; crossed □ for LAC, LYS, and RIB). Bands in this frequency range may be attributed to β-turn, 3_{10}-helix, or a high-frequency component of inter- or intramolecular β-sheet. Except for RIB, these bands show an increasing

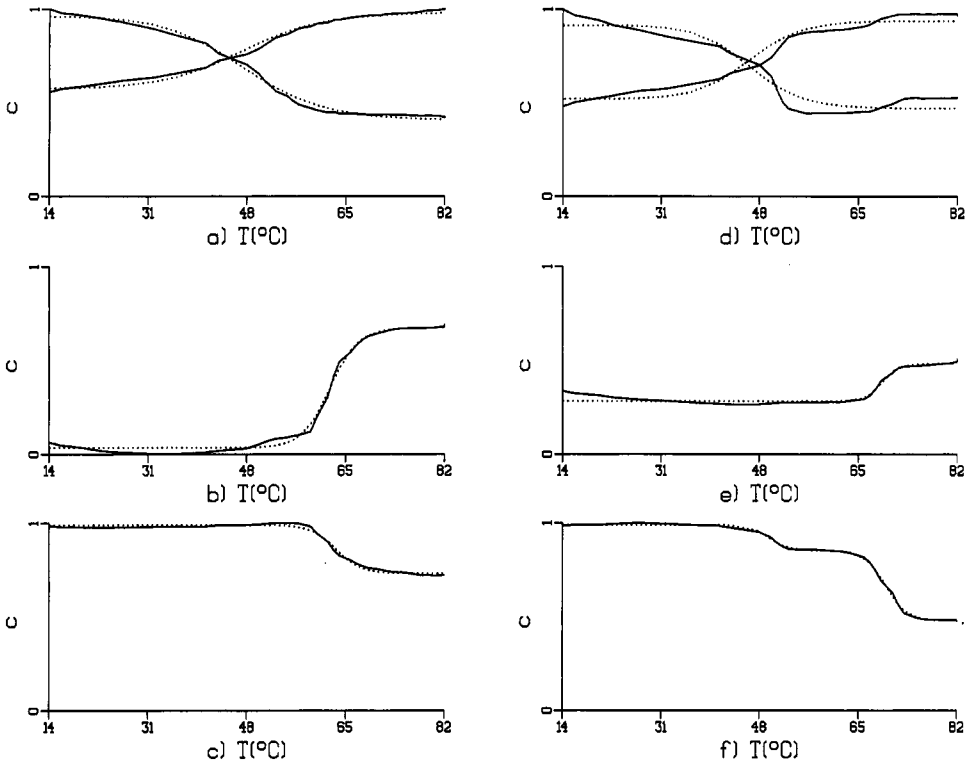

FIGURE 4: Fits of some of the c (T) curves of ALB (a−c) and LYS (d−f) according to eq 3. Parameters can be found in Table 2. (a, d) $^1H-^2H$ exchange; (b, e) increase in intermolecular β-sheet; (c, f) decrease of intramolecular secondary structure. Solid lines represent estimated c (T) curves, whereas the dotted lines show the fit according to eq 3.

transition upon heating that coincides with the increase in the 1616−1620-cm^{-1} band (intermolecular β-sheet) and a gradual decrease during cooling. Hence, it seems obvious that molecular aggregation contributes to this band. However, its behavior upon cooling, and the occurrence of additional bands in the second derivative and deconvoluted spectra of this region (Table 1), suggests that multiple bands are averaged. More detailed analysis is required.

The thermal behavior of RIB (Figure 3p,q,r) is different from that of all other proteins studied except for the $^1H-^2H$ exchange transition, which is, as expected, irreversible. Its intramolecular β-sheet (1635 cm^{-1}, ◇ in Figure 3q,r) and other bands (1674, 1654, and 1625 cm^{-1}) show transitions that are more or less reversible upon cooling. Moreover, rather than forming intermolecular β-sheet structure, RIB forms another form of structure, possibly "random coil", giving rise to a broad feature in the region of 1654 cm^{-1} (▽ in Figure 3q,r), whereas all the other bands are lost. The 1625-cm^{-1} band may arise from amino-acid side chains whose hydrogen bonding is disrupted and reformed. Alternatively, it may be non-well-defined secondary structure which is broken upon heating.

Thermodynamic Fit of Band Amplitude Curves. Although formally the application of eq 3 is only allowed for a real two-state fully reversible transition (Elwell & Schellman, 1977), and the here-described transitions surely do not fulfill these conditions entirely, we fitted the heating parts of the band-amplitude curves (Figure 3), which showed a sigmoidal progression, with eq 3. In the 1420−1600-cm^{-1} range the heating parts of the $c(T)$ curves of the amide II and amide II′ bands could be reasonably well fitted globally with eq 3 [compare the dotted lines of the fit with the solid lines of the $c(T)$ curves in Figure 4a,d], resulting in the midpoint temperatures T_m of Table 2. In this fit the increase in amide II′ and decrease in amide II were fitted together. In the 1600−1720-cm^{-1} range we separately fitted the increase in the 1620-cm^{-1} band (intermolecular structure) and the decrease of the 1638−1656-cm^{-1} region (intramolecular structure). The results for ALB and LYS are shown, respectively, in panels b and e and panels c and f of Figure 4. Note that the T_m of the two transitions observed in Figure 4f coincide with, respectively, the T_m of $^1H-^2H$ exchange (Figure 4d) and of aggregation (Figure 4e). As Table 2 (columns 3 and 4) shows, the estimated midpoint temperatures T_m of aggregation and intramolecular secondary structure decrease are almost identical for each protein except FIB. The last column of Table 2 gives the van't Hoff enthalpy ΔH_m for the intramolecular secondary structure decrease. The ΔH_m parameters of $^1H-^2H$ exchange and aggregation are not given because we have no physical interpretation for these.

Table 2: Parameters of Fit of Band Amplitude Curves c (T) According to eq 3[a]

protein	T_m for $^1H-^2H$ exchange[b] (°C)	T_m for amide I′ increase[c] (°C)	T_m for amide I′ decrease[d] (°C)	ΔH_m (kJ/mol)[d]
ALB	47.4 (4)	62.4 (2)	63.4 (3)	438 (39)
FIB	43 (2)	*e*	*e*	*e*
IgG	63 (2)	68.3 (3)	69.3 (3)	251 (14)
LAC	43.9 (3)	64 (2)	63.5 (4)[f]	208 (15)[f]
LYS	46.3 (8)		49.7 (3)[g]	531 (82)
		69.2 (4)	70 (1)[g]	542 (25)
RIB	37.7 (4)	52.0 (2)	52.6 (3)	268 (19)

[a] Numbers in parentheses indicate the error in the last digit. [b] Amide II and amide II′ bands; cf. Figure 4a,d. [c] Intermolecular β-sheet band; cf. Figure 4b,e. [d] Intramolecular secondary structure band; cf. Figure 4c,f. [e] Curve could not be fitted well with the model of Eq. 3. [f] Curve fitted from 50 to 82 °C. [g] Two transitions, cf. Figure 4f.

DISCUSSION

Global Analysis. In Table 1 we compare the bands obtained from global analysis with those found by second derivative and deconvolution at 14 and 82 °C. Between 1500 and 1600 cm^{-1}, the 1516-cm^{-1} band (tyrosine) and the band around 1580 cm^{-1} (carboxylate) are found by all methods. The amide II region, which is represented by a single band at 1545 cm^{-1} in the global analysis, shows two bands between 1530 and 1550 cm^{-1} in second derivative/deconvolution. Moreover, the latter methods sometimes give an extra band around 1570 cm^{-1}, which seems to have merged with the carboxylate band in global analysis.

In the 1600−1700-cm^{-1} range, eight bands are discriminated in second-derivative and deconvoluted spectra. In the global analysis the small 1600−1614-cm^{-1} band is integrated in the 1616−1620-cm^{-1} band (aggregation), and the secondary-structure bands between 1630 and 1675 cm^{-1} are merged into one or two bands. The high-energy band around 1680 cm^{-1} is found in both global analysis and second derivative/deconvolution.

From the comparison between second derivative/deconvolution and global analysis it is clear that the latter is less appropriate for a detailed detection of all bands occurring in the FTIR spectra, and neither is it meant to be used to this end. The global analysis was developed as a method to analyze spectral changes as a function of an independent parameter in a quantitative and statistically reliable way. Currently used methods for FTIR spectra analysis, like second derivative and deconvolution, are less suitable to this end. We are interested in deducing temperature-induced structural changes in proteins from their FTIR spectra, and we applied the global analysis with the minimum numbers of bands. Table 1 shows that the major features of the spectra as found by deconvolution and second derivative are also found by the global analysis. As explained above, we performed the global analysis with a minimum number of bands in order to prevent artifacts. This implies that minor bands are not taken into consideration and that strongly overlapping bands with comparable temperature dependence will be fitted with a single averaged band. When overlapping bands have a significantly different temperature profile, the global analysis will separate them.

A crucial assumption of eq 1 is the temperature independence of the shape of the absorption bands. In general, increasing temperature can give rise to band broadening as well as shifts caused by changes in hydrogen bonding. These violations will give rise to structured residuals, as they are present, albeit small, in Figure 2. Notwithstanding these limitations, we conclude that the global analysis is a reliable method to identify temperature-induced global changes in FTIR spectra and hence in protein conformation. As we will show below, it also allows estimation of some thermodynamic parameters of the conformational change. However, it does not enable a detailed quantification of changes in secondary-structure content.

Transition Temperature and van't Hoff Enthalpies. In the van't Hoff analysis it is implicitly assumed that there are only two thermodynamically identifiable states and that unfolding is fully reversible (Elwell & Schellman, 1977). This applies for RIB, but it is obviously not the case when unfolding is accompanied by intramolecular aggregation. However, reasonable van't Hoff plots are often observed in cases of apparently irreversible denaturation, which might provide a measure of validity to the application of equilibrium thermodynamics to irreversible processes in proteins (Sturtevant, 1987). In order to check whether the T_m and ΔH_m values corresponding to the secondary-structure decrease collected in Table 2 (columns 4 and 5) comply with Sturtevant's observation and have physical relevance and reliability, we compare them with literature values for T_m and the van't Hoff enthalpy (ΔH_{vH}), which are collated in Table 3. The $^1H-^2H$ exchange-related parameters will be discussed below. For IgG the van't Hoff enthalpy has not been measured before, whereas the relevant transition for FIB is above the temperature we could measure by FTIR. In the case of LYS we consider the second transition (see Figure 4f), since the first one is likely to be an artifact due to $^1H-^2H$ exchange, as discussed above.

Table 3: Literature Values of Thermodynamic Parameters

protein	T_m for denaturation (°C)	ΔH_{cal} (kJ/mol)	ΔH_{vtHoff} (kJ/mol)
ALB	63.1[a]	1150[b]	675[a]
FIB	45, 90.5, 95[c]; 56, 95[d]	2362, 2236[c]; 3352, 1304[d]	652, 928[d]
IgG	63.9, 64.9, 69.2, 72.5, 80.4[e]	681, 882, 773, 807, 497[e]	
LAC	57;[f] 62[g]		230;[f] 238[g]
LYS	76.5;[h] 77;[i] 72.5;[j] 75[k]	577;[h] 489[j]	514;[h] 460;[i] 523[k]
RIB	48;[l] 46;[m] 46[n]	447[n]	355;[l] 326;[m] 280[n]

[a] Ross and Shrake (1988); pH 7.0, 150 mM NaCl. [b] Shrake and Ross (1988); pH 7.0, 150 mM NaCl. [c] Procyk et al. (1992); pH 3.5, 0.05 M glycine. ΔH_{cal} of 90.5, 95 °C combined. [d] Privalov and Medved (1982); pH 8.5. [e] Buchner et al. (1991); murine κ/IgG_1, pH 7.0, deconvoluted. [f] Barel et al. (1972); pH 8.1, 0.1 M Tris. [g] Permyakov et al. (1985); pH 8.0, 50 mM Hepes. [h] Delben and Crescenzi (1969); pH 5.4, 0.1 M phosphate. [i] Dobson and Evans (1984); pH 3.8. [j] Fujita and Noda (1992); pH 3, 0.05 M glycine. [k] Hamaguchi and Sakai (1965). [l] Tsong et al. (1970); pH 7, 0.2 M NaCl. [m] Labhardt (1981); pH 7. [n] Hearn et al. (1971); pH 7, 0.3 M NaCl.

For the comparison of these values, the following points should be realized. (a) Both the transition temperature and enthalpy often depend strongly on pH, ionic strength, and the type of salt present in the solution [see, e.g., Scott and Scheraga (1963), Tanford (1968), and Yamasaki et al. (1991)]. (b) Small shifts in the amide I band due to $^1H-^2H$ exchange during unfolding of the secondary structure may affect values calculated in ^2H_2O slightly.

T_m values are usually close to the reported values. The van't Hoff enthalpies of LAC and LYS are in good agreement. Those of ALB and RIB are 20−35% lower than the previously observed values. Therefore we conclude that, notwithstanding violation of one of the basic assumptions of the two-state model, *viz.* reversibility of the transitions, the deduced thermodynamic values in many cases have reasonable reliability, as observed before by Sturtevant (1987).

Multiple Domains in ALB, FIB, IgG, and RIB. Having established in the previous section that the thermodynamic parameters found in this study have reasonable reliability, we will analyze them in some more detail. The van't Hoff enthalpy is only equal to the calorimetric enthalpy for a single two-state transition. For n independently denaturing domains, $\Delta H_{cal}/\Delta H_{vH}$ equals n. Interaction lowers this ratio (Tanford, 1968; Privalov, 1982).

When we combine our value of ΔH_m for ALB with the calorimetric enthalpy (ΔH_{cal} column of Table 3), $\Delta H_{cal}/\Delta H_m$ is 2.6 ± 0.3. This value can be explain by the presence of three homologous domains in albumin (He & Carter, 1992). The value of 2.6 instead of 3 could indicate some interaction between the domains. Indeed, Tiktopulo et al. (1985) found three overlapping transitions after deconvolution of the differential scanning calorimetric thermogram of human serum albumin (pH 7.0, 100 mM phosphate).

Fibrinogen at pH 8.5 has a low-temperature transition that corresponds to melting of the low-structured, globular carboxyl-terminal parts of the subunits and a high-temperature one corresponding to melting of the central globular structure and the coiled-coil regions in the end domains. At low pH the latter is split into two transitions (Privalov & Medved, 1982; Procyk et al., 1992). Neither of the transitions is observed by our FTIR spectroscopy method. The high-temperature transition is above our temperature range, whereas the low-temperature transition does not involve a clear secondary-structure change as reflected in a modification of the amide I absorption.

Although both fluorescence spectroscopy and differential scanning calorimetry of IgG at pH 7.4 (0.15 M NaCl, 0.02 M phosphate) give apparently a single transition between 63 and 73 °C (Brandau et al., 1991), the denaturation behavior of immunoglobulins is somewhat complicated (Privalov, 1982). Buchner et al. (1991) find three overlapping transitions at pH 7.0 for MAK33, a murine antibody of subtype κ/IgG$_1$. Direct comparison between their values and our from human IgG cannot be made. However, the ratio of the total calorimetric enthalpy found by them and our ΔH_m value is about 15. Tischenko et al. (1982) find 12 different domains in IgG. The values of T_m and ΔH_m for (the single-domain protein) human α-lactalbumin are close to the calorimetric values found for bovine α-lactalbumin [T_m = 62.0 ± 0.2 °C, ΔH_{cal} = 276 kJ/mol, $\Delta H_{cal}/\Delta H_{vH}$ = 1.06 (Pfeil, 1981)].

The ratio between ΔH_m of RIB and the calorimetric value from Table 3 is about 2. This may point to two independently denaturing structural regions in RIB. Two parallel independent transitions in different regions have also been observed for ribonuclease A (Scott & Scheraga, 1963).

Hydrogen−Deuterium Exchange. Figures 3 and 4a,d show that, except in the case of FIB, the ^{1}H−^{2}H exchange proceeds more or less sigmoidally with increasing temperature. The estimated midpoint temperature T_m of ^{1}H−^{2}H exchange varies from 38 °C for RIB to 47 °C for ALB (Table 2), whereas in the case of IgG the temperature trajectories of exchange and secondary-structure denaturation overlap. Enhanced exchange upon heating can be caused by increased kinetic energy of the NH bonds without structural changes in the proteins. However, this is not likely to be the dominating effect in our case, as this would result in a gradual rather than a sigmoidal dependence on temperature.

Two inhibitions for ^{1}H−^{2}H exchange in native proteins have been observed, viz., strong hydrogen bonding in secondary structure and inaccessibility to the solvent due to tertiary structure (Benson, 1964; Englander & Kallenbach, 1984; Rashin, 1987; Pedersen et al., 1991; Englander & Englander, 1994). Accordingly, enhanced exchange under destabilizing conditions has been explained by either local unfolding or increased solvent penetration (Englander & Kallenbach, 1984). Englander and Kallenbach conclude that in most cases intramolecular hydrogen bonding provides the main blockage for ^{1}H−^{2}H exchange but that in some cases solvent accessibility is the dominating factor. On the basis of our data we feel not justified to decide between these two mechanisms. In the next section we discuss literature which supports the interpretation of the enhanced exchange in terms of increased solvent penetration.

Folding Intermediates. Two types of folding intermediates exist: (i) kinetic ones that occur during folding and unfolding of proteins but do not exist long enough to be isolated and (ii) equilibrium intermediates, which form the majority of the molecular conformation of a protein under certain conditions (Kuwajima et al., 1985). Some of these have a more or less native secondary structure but a collapsed or highly flexible tertiary structure leading to enhanced hydrogen exchange (Kuwajima et al., 1985; Creighton, 1990; Ptitsyn et al., 1990; Ewbank & Creighton, 1993a,b). For the proteins used in this study, stable folding intermediates have been inferred for ALB at low pH (Benson et al., 1964; Buchner et al., 1991) or elevated temperature (Lin & Koenig, 1976), LAC in low concentrations of guanidine hydrochloride, at low pH, or at elevated temperature (Kuwajima et al., 1985; Pfeil, 1981), and IgG at low pH (Buchner et al., 1991). For LYS and RIB, only kinetic intermediates have been described (Kim & Baldwin, 1982; Ikeguchi et al., 1986; Miranker et al., 1991). As Table 2 and Figure 3 show, we observe an enhanced hydrogen exchange without concomitant secondary structure change for all the proteins studied except perhaps IgG. We attribute this to a partially unfolded state with intact secondary structure and collapsed or highly flexible tertiary structure. The transition temperature for the proposed folding intermediate of ALB corresponds well with that found by Lin and Koenig (1976), who observed a reversible conformational change at 42 °C where the secondary structure remained but the tertiary structure became loose. This once more illustrates the reliability and value of FTIR combined with global analysis for the study of temperature-induced structural changes in proteins. For LYS and RIB this would be the first description of an apparently stable folding intermediate in aqueous solution; however, in contradistinction to this study, most of the measurements on LYS reported in the literature have been performed at low pH. A state with intact secondary and changed tertiary structure has been observed for LYS in 15% 2,2,2-trifluoroethanol at pH 2.0 (Buck et al., 1993), and a quasistable intermediate state for LYS has been deduced from molecular dynamics calculations (Mark & van Gunsteren, 1992). Khechinashvili et al. (1973) found no intermediate thermodynamically stable state for LYS but observed a predenaturation change in the heat capacity.

Perhaps the intermediate form found by us is related to the pre-molten globule state as described by Lala and Kaul (1992). Some support for the formation of this type of folding intermediates can be found. Nakanishi et al. (1973) combined ^{1}H−^{2}H exchange measurements with IR and UV absorption and found that between 25 and 50 °C LYS is in equilibrium with another sort of unfolded form than between 65 and 85 °C. Khechinashvili et al. (1973) and Privalov (1979) observed a predenaturational stage where there is a change in heat capacity probably connected with labilization of the globule structure. It was concluded that the predenaturational change involved enhanced solvent accessibility. The authors could not conclude whether the change in state

was continuous or abrupt. Wedin et al. (1982) found that LYS shows enhanced $^1H-^2H$ exchange of the tryptophan indole NH about 15 °C below the regular denaturation temperature and ascribed this to enhanced flexibility. Delepierre et al. (1987) observed that $^1H-^2H$ exchange takes place from a conformation of the protein closely similar to that of the native protein. The fact that this type of folding intermediate has hardly been observed before might be caused by the different salt and pH conditions generally used for folding intermediate studies.

Recently, the significance of partially folded intermediates has been questioned, and it has been argued that they arise from kinetically trapped misfolded proteins that are not part of the intrinsic folding process (Sosnick et al., 1994). Counterarguments have been presented by Creighton (1994). One of the main arguments of Sosnick et al. is that folding intermediates are the result of specific solution conditions, whereas they are not observed when these conditions are properly adjusted. In our case, measurements have been performed in physiological salt solution, which we believe to be the optimal system to study protein folding in conditions as close as possible to real life. Moreover, Creighton (1994) has noted that the nature of the overall transition state for folding is best characterized by monitoring unfolding rather than folding, which is the approach we have followed.

Summary and Conclusions. In this paper we analyze FTIR spectra as a function of a variable parameter, in particular the temperature. To do this we introduce a new method, based on global analysis. This method has the advantage that no data preprocessing is required, which implies that no information is lost. In this case the spectra were analyzed with the minimum number of bands necessary for a proper fit. As a consequence, strongly overlapping bands with the same amplitude variation as a function of the temperature will be fitted with a single band. Although this had the disadvantage that in some cases the changes in different secondary structure elements were not separately monitored, it prevented the introduction of artifacts due to overfitting of the data. Moreover, our intent in this paper was to identify global secondary or tertiary structure changes rather than to quantify changes in the secondary structure content. If different types of secondary structure have a different temperature dependence, it will be observed even in the case of strong band overlap. The estimated band amplitudes as a function of temperature obtained from the global analysis were subsequently (globally) fitted with a two-state thermodynamic model. Transition enthalpies and midpoint temperatures so obtained compare well with published literature values.

The results point to a change in tertiary structure leading to enhanced solvent accessibility followed by a secondary structure unfolding accompanied by protein aggregation at a higher temperature. The aggregation is enhanced during subsequent cooling. For some of the proteins in this study, the first structural change takes place at a temperature slightly above the physiological temperature of 37 °C, which might imply a physiological significance. A more detailed analysis requires a comparison with analogous experiments in ^1H_2O. Such measurements and analyses are in progress.

ACKNOWLEDGMENT

The valuable advice of R. J. Heaton is gratefully acknowledged. F. C. A. Groen and W. D. Hoff are thanked for critical reading of the text and helpful discussion.

SUPPORTING INFORMATION AVAILABLE

Table 1S, containing spectral parameters of FTIR absorption bands fitted according to eq 2 (location $\bar{\nu}_{max}$, width $\Delta\bar{\nu}$, and skewness b); in addition, symbols referring to Figure 3 and band assignment are given (1 page). Ordering information is given on any current masthead page.

REFERENCES

Arrondo, J. L. R., Muga, A., Castresana, J., & Goñi, F. M. (1993) *Prog. Biophys. Mol. Biol. 59*, 23−56.
Azpiazu, I., & Chapman, D. (1992) *Biochim. Biophys. Acta 1119*, 268−274.
Baldwin, R. L. (1990) *Nature 346*, 409−410.
Barel, A. O., Prieels, J. P., Maes, E., Looze, Y., & Leonis, J. (1972) *Biochim. Biophys. Acta 257*, 288−296.
Benson, E. S., Hallaway, B. E., & Lumry, R. W. (1964) *J. Biol. Chem. 239*, 122−129.
Brandau, D. T., Lawson, E. Q., Schubert, C. F., Day, N. K., Matsuno, K., & Middaugh, C. R. (1991) *Mol. Immunol. 28*, 1019−1026.
Buchner, J., Renner, M., Lilie, H., Hinz, H. J., Jaenicke, R., Kiefhabel, T., & Rudolph, R. (1991) *Biochemistry 30*, 6922−6929.
Buck, M., Radford, S. E., & Dobson, C. M. (1993) *Biochemistry 32*, 669−678.
Casal, H. L., Köhler, U., & Mantsch, H. H. (1988) *Biochim. Biophys. Acta 957*, 11−20.
Chirgadze, Yu. N., Fedorov, O. V., & Trushina, N. P. (1975) *Biopolymers 14*, 679−694.
Clark, A. H., Saunderson, D. H. P., & Suggett, A. (1981) *Int. J. Pept. Protein Res. 17*, 353−364.
Creighton, T. E. (1990) *Biochem. J. 270*, 1−16.
Creighton, T. E. (1994) *Nature, Struct. Biol. 1*, 135−138.
Delben, F., & Crescenzi, V. (1969) *Biochim. Biophys. Acta 194*, 615−618.
Delepierre, M., Dobson, C. M., Karplus, M., Poulsen, F. M., States, D. J., & Wedin, R. E. (1987) *J. Mol. Biol. 197*, 111−130.
Dobson, C. M., & Evans, P. A. (1984) *Biochemistry 23*, 4267−4270.
Dolgikh, D. A., Gilmashin, R. I., Brazhnikov, E. V., Bychkova, V. E., Semisotnov, G. V., Venyaminov, S. Y., & Ptitsyn, O. B. (1981) *FEBS Lett. 136*, 311−315.
Elwell, M. L., & Schellman, J. A. (1977) *Biochim. Biophys. Acta 494*, 367−383.
Englander, S. W., & Kallenbach, N. R. (1984) *Q. Rev. Biophys. 16*, 521−655.
Englander, S. W., & Englander, J. J. (1994) *Methods Enzymol. 232*, 26−42.
Ewbank, J. J., & Creighton, T. E. (1993a) *Biochemistry 32*, 3677−3693.
Ewbank, J. J., & Creighton, T. E. (1993b) *Biochemistry 32*, 3694−3707.
Fraser, R. D. B., & Suzuki, E. (1969) *Anal. Chem. 41*, 37−39.
Fujita, Y., & Noda, Y. (1992) *Int. J. Pept. Protein Res. 40*, 103−109.
Griffiths, P. R., & Haseth, J. A. (1986) *Fourier Transform Infrared Spectrometry*, pp 17−23, Wiley, New York.
Hadden, J. M., Bloemendal, M., Haris, P. I., Srai, K. S., & Chapman, D. (1994a) *Biochim. Biophys. Acta 1205*, 59−67.
Hadden, J. M., Bloemendal, M., Haris, P. I., Van Stokkum, I. H. M., Chapman, D., & Srai, S. K. S. (1994b) *FEBS Lett. 350*, 235−239.
Hamaguchi, K., & Sakai, H. (1965) *J. Biochem. (Tokyo) 57*, 721−732.
Haris, P. I., & Chapman, D. (1992) *Trends Biochem. Sci. 17*, 328−333.

Haris, P. I., Lee, D. C., & Chapman, D. (1986) *Biochim. Biophys. Acta 874*, 255−265.
He, X. M., & Carter, D. C. (1992) *Nature 358*, 209−215.
Hearn, R. P., Richards, F. M., Sturtevant, J. M., & Watt, G. D. (1971) *Biochemistry 10*, 806−817.
Igarashi, T., Sato, M., Katsube, Y., Takio, K., Tanaka, T., Nakanishi, M., & Arata, Y. (1990) *Biochemistry 29*, 5727−5733.
Ikeguchi, M., Kuwajima, K., Mitani, M., & Sugai, S. (1986) *Biochemistry 25*, 6965−6972.
Khechinashvili, N. N., Privalov, P. L., & Tiktopulo, E. I. (1973) *FEBS Lett. 30*, 57−60.
Kim, P. S., & Baldwin, R. L. (1982) *Annu. Rev. Biochem. 51*, 459−489.
Kirsch, J. L., & Koenig, J. L. (1989) *Appl. Spectrosc. 43*, 445−451.
Kuwajima, K., Hiraoka, Y., Ikeguchi, M., & Sugai, S. (1985) *Biochemistry 24*, 874−881.
Labhardt, A. M. (1981) *Biopolymers 20*, 1459−1480.
Lala, A. K., & Kaul, P. (1992) *J. Biol. Chem. 267*, 19914−19918.
Levitt, M., & Greer, J. (1977) *J. Mol. Biol. 114*, 181−239.
Lin, V. J. C., & Koenig, J. L. (1976) *Biopolymers 15*, 203−218.
McKenzie, H. A., & White, F. H., Jr. (1991) *Adv. Protein Chem. 41*, 173−315.
Mark, A. E., & van Gunsteren, W. F. (1982) *Biochemistry 31*, 7745−7748.
Miranker, A., Radford, S. E., Karplus, M., & Dobson, C. M. (1991) *Nature 349*, 633−636.
Muga, A., Mantsch, H. H., & Surewicz, W. K. (1991) *Biochemistry 30*, 7219−7224.
Murphy, K. P., & Freire, E. (1992) *Adv. Protein Chem. 43*, 313−361.
Nakanishi, M., Tsuboi, M., & Ikegami, A. (1973) *J. Mol. Biol. 75*, 673−682.
Pace, C. N., Shirley, B. A., & Thomson, J. A. (1989) in *Protein structure, a practical approach* (Creighton, T. E., Ed.) pp 311−330, IRL Press, Oxford, England.
Pain, R. H. (1992) *Nature 358*, 278−279.
Pandya, B. V., Cierniewski, C. S., & Budzynski, A. Z. (1985) *J. Biol. Chem. 260*, 2994−3000.
Pedersen, T. G., Sigurskjold, B. W., Andersen, K. V., Kjaer, M., Poulsen, F. M., Dobson, C. M., & Redfield, C. (1991) *J. Mol. Biol. 218*, 413−426.
Permyakov, E. A., Morozova, L. A., & Burstein, E. A. (1985) *Biophys. Chem. 21*, 21−31.
Pfeil, W. (1981) *Biophys. Chem. 13*, 181−186.
Prestrelski, S. J., Byler, D. M., & Liebman, M. N. (1991a) *Biochemistry 30*, 133−143.
Prestrelski, S. J., Byler, D. M., & Thompson, M. P. (1991b) *Biochemistry 30*, 8797−8804.
Privalov, P. L. (1979) *Adv. Protein Chem. 33*, 167−241.
Privalov, P. L. (1982) *Adv. Protein Chem. 35*, 1−104.
Privalov, P. L., & Medved, L. V. (1982) *J. Mol. Biol. 159*, 665−683.
Procyk, R., Medved, L., Engelke, K. J., Kudryk, B., & Blombäck, B. (1992) *Biochemistry 31*, 2273−2278.
Ptitsyn, O. B., Pain, R. H., Semisotnov, G. V., Zerovnik, E., & Razgulyaev, O. I. (1990) *FEBS Lett. 262*, 20−24.
Rashin, A. A. (1987) *J. Mol. Biol. 198*, 339−349.
Ross, P. D., & Shrake, A. (1988) *J. Biol. Chem. 263*, 11196−11202.
Scott, R. A., & Scheraga, H. A. (1963) *J. Am. Chem. Soc. 85*, 3866−3873.
Sevilla, J. M., Dominguez, M., Garcia-Blanco, F., & Blazquez, M. (1989) *Comput. Chem. 13*, 197−200.
Shrake, A., & Ross, P. D. (1988) *J. Biol. Chem. 263*, 15392−15399.
Sosnick, T. R., Mayne, L., Hiller, R., & Englander, S. W. (1994) *Nature, Struct. Biol. 1*, 149−156.
Sturtevant, J. M. (1987) *Annu. Rev. Phys. Chem. 38*, 463−488.
Surewicz, W. K., Mantsch, H. H., Chapman, D. (1993) *Biochemistry 32*, 389−394.
Susi, H., & Byler, D. M. (1986) *Methods Enzymol. 130*, 290−311.
Tanford, C. (1968) *Adv. Protein Chem. 23*, 121−282.
Tiktopulo, E. I., Privalov, P. L., Borisenko, S. N., & Troitskii, G. V. (1985) *Mol. Biol. (Moscow) 19*, 1072−1078.
Tischenko, V. M., Zav'yalov, V. P., Medgyesi, G. A., Potekhin, S. A., & Privalov, P. L. (1982) *Eur. J. Biochem. 126*, 517−521.
Tsong, T. Y., Hearn, R. P., Wrathall, D. P., & Sturtevant, J. M. (1970) *Biochemistry 9*, 2666−2677.
Van Stokkum, I. H. M., Scherer, T., Brouwer, A. M., & Verhoeven, J. W. (1994) *J. Phys. Chem. 98*, 852−866.
Venyaminov, S. Yu., & Kalnin, N. N. (1990) *Biopolymers 30*, 1243−1257.
Wedin, R. E. Delepierre, M., Dobson, C. M., & Poulsen, F. M. (1982) *Biochemistry 21*, 1098−1103.
Xie, D., Bhakuni, V., & Freire, E. (1991) *Biochemistry 30*, 10673−10678.
Yamasaki, M., Yano, H., & Aoki, K. (1991) *Int. J. Biol. Macromol. 13*, 322−328.
Yang, P. W., Matsch, H. H., Arrondo, J. L. R., Saint-Girons, I., Guillou, Y., Cohen, G. N., & Bârzu, O. (1987) *Biochemistry 26*, 2706−2711.
Zuber, G., Prestrelski, S. J., & Benedek, K. (1992) *Anal. Biochem. 207*, 150−156.

BI941972K